HHS Public Access

Author manuscript

Radiother Oncol. Author manuscript; available in PMC 2018 July 01.

Published in final edited form as:

Radiother Oncol. 2017 July ; 124(1): 168–173. doi:10.1016/j.radonc.2017.05.013.

An evaluation of motion mitigation techniques for pancreatic SBRT

Warren G. Campbell, **Bernard L. Jones**, **Tracey Schefter**, **Karyn A. Goodman**, and **Moyed Miften**

Department of Radiation Oncology, University of Colorado School of Medicine, Aurora, CO 80045, USA

Abstract

Background and purpose—Ablative radiation therapy can be beneficial for pancreatic cancer, and motion mitigation helps to reduce dose to nearby organs-at-risk. Here, we compared two competing methods of motion mitigation—abdominal compression and respiratory gating.

Materials and methods—CBCT scans of 19 pancreatic cancer patients receiving stereotactic body radiation therapy were acquired with and without abdominal compression, and 3D target motion was reconstructed from CBCT projection images. Daily target motion without mitigation was compared against motion with compression and with simulated respiratory gating. Gating was free-breathing and based on an external surrogate. Target coverage was also evaluated for each scenario by simulating reduced target margins.

Results—Without mitigation, average daily target motion in LR/AP/SI directions were 5.3, 7.3, and 13.9 mm, respectively. With abdominal compression, these values were 5.2, 5.3, and 8.5 mm, and with respiratory gating they were 3.2, 3.9, and 5.5 mm, respectively. Reductions with compression were significant in AP/SI directions, while reductions with gating were significant in all directions. Respiratory gating also demonstrated better coverage in the reduced margins scenario.

Conclusion—Respiratory gating is the most effective strategy for reducing motion in pancreatic SBRT, and may allow for dose escalation through a reduction in target margin.

Keywords

Pancreatic SBRT; Motion management; Respiratory gating; Abdominal compression

Pancreatic cancer remains an oncologic challenge, with only a minority of patients who can undergo curative resection. The role of standard, long-course chemoradiation in the

Corresponding author: Warren G. Campbell, Department of Radiation Oncology, University of Colorado School of Medicine, 1665 Aurora Court, Suite 1032 – MS F706, Aurora, CO 80045, USA, Phone: 1-250-508-3419, warren.campbell@ucdenver.edu.

Conflict of interest statement: The University of Colorado and authors Campbell, Jones, and Miften have filed a provisional patent application for the fiducial marker tracking technique used in this work.

management of locally advanced, unresectable disease is controversial based on recent Phase III data [1]. In recent years, an ablative form of radiotherapy known as stereotactic body radiation therapy (SBRT) has emerged as an attractive option for patients with locally advanced pancreatic cancer [2-6].

With added emphasis on precision and accuracy, SBRT allows for high doses to be delivered in shorter fractionation schedules. To administer SBRT safely, three main challenges should be considered. First, the stomach and duodenum are highly radiosensitive and sit directly adjacent to the pancreas, so particular care must be taken to limit unnecessary exposure to these organs-at-risk (OARs) [7-10]. Second, poor contrast in kilovoltage imaging makes daily localization of tumors challenging, so fiducial markers are typically used to allow for accurate localization prior to each treatment [11]. Third, the pancreas is susceptible to motion caused by breathing, digestion, and heartbeat. Consequently, motion mitigation is a vital component of pancreatic SBRT.

In general, reducing target volumes is a primary goal in pancreatic SBRT. In 2005, the Hoyer *et al* trial used target volumes that were large compared to similar trials, and their rate of gastrointestinal toxicity was extremely high [10]. Recently, Brunner *et al* demonstrated that there is still room for improvements to local control through dose escalation with SBRT, but smaller target volumes are necessary to ensure acceptably low rates of toxicity [9]. Better motion mitigation techniques could allow for target volumes to be reduced.

Two methods of motion mitigation are commonly used for pancreatic SBRT: abdominal compression and respiratory gating. Abdominal compression involves applying pressure to the patient's abdomen to limit diaphragmatic motion, thereby reducing target motion. Primary drawbacks to abdominal compression include causing the patient undue pain or discomfort, and potentially pushing OARs closer to the target volume. Respiratory gating typically involves the use of an external surrogate whose motion is correlated with internal tumor motion, and the treatment beam is only activated during a specific phase of the breathing cycle. The primary drawback to respiratory gating is the lengthening of treatment times, although these can be accounted for by using high dose-rate, flattening-filter free beams. Another common technique requires that the patient hold their breath during treatment; however, this has been shown to have poor accuracy for pancreatic tumors [12]. Other methods attempt to track the tumor directly without the use of an external surrogate [13,14].

This study investigates the efficacy of abdominal compression and respiratory gating for reducing target motion in pancreatic SBRT. Ranges of daily 3D target motion were measured and compared for three motion scenarios: no motion mitigation, abdominal compression, and respiratory gating. In addition to examining ranges of daily target motion, a simulated clinical scenario with reduced internal target volume margins was used to illustrate how each approach can influence target coverage. By determining the best technique for motion mitigation, there is greater potential for dose escalation to the primary tumor and improved patient outcomes.

Methods

Patients

Nineteen consecutive patients with cancer of the pancreas (15 head, 4 body) received SBRT treatment between July 2015 and May 2016 at our institution. To aid with daily target localization, each patient had 3 to 4 radio-opaque fiducial markers (carbon-coated titanium, cylindrical, 1 mm diameter, 5 mm long) implanted in or near their tumor using endoscopic ultrasound guidance. Then, computed tomography (CT) simulations were used to acquire two sets of data for treatment planning purposes: a 3D CT scan for dose calculation, and a 4DCT scan to assess respiratory motion. For the 4DCT scan, an external block with infrared markers (i.e., an external surrogate) was tracked to allow for CT data to be reconstructed according to breathing phase.

Patients were prescribed to receive a total of 30-33 Gy in five treatment fractions. Internal target volumes (ITVs) were selected to encompass the full range of clinical target volume (CTV) motion observed in the 4DCT scan. Physicians then expanded ITVs on a case-by-case basis using patient-specific anisotropic margins of up to 5 mm, resulting in the planning target volume (PTV).

During simulation and treatment, tumor motion was mitigated using abdominal compression (SBRT Solution Pressure Belt, ORFIT Industries, Wijnegem, Belgium; Respiratory Compression Belt, Aktina Medical, Congers, NY, USA). Belt pressure settings were determined for each patient individually prior to CT simulation by inflating the belt until the patient began to feel pain or discomfort. Pressure settings determined at simulation were reproduced for each treatment using a belt of the same make and model.

Daily imaging

For the purposes of this study, motion observed at simulation was not used to evaluate motion mitigation techniques. Previous studies have demonstrated discrepancies between the abdominal target motion observed by 4DCT at simulation and the day-to-day motion observed for the same patients at the treatment table [15-18]. Due to such discrepancies, more comprehensive techniques for motion evaluation are required [19]. We have developed and implemented an in-house motion reconstruction technique to accurately determine daily tumor motion (described below) [20]. As such, motion measurements for this work were obtained by cone-beam CT (CBCT) imaging just prior to treatment.

As part of routine treatment, CBCT scans were acquired by the linear accelerator's on-board imager just prior to each treatment fraction while the patient wore the abdominal compression belt. Three-dimensional volumes provided by these scans were used to re-position the patient prior to treatment. During each 1-minute scan, 892 projection images were collected across a full gantry rotation at a rate of 14.8 images per second. Images had a resolution of 768×1024, with square pixels 0.388 mm in size (0.259 mm projected at the isocenter).

For the purposes of this study, additional CBCT scans were acquired for a subset of treatments while patients were not wearing the abdominal compression belt. These

uncompressed scans were acquired just prior to the routine, compressed scan. During uncompressed scans, breathing data was also collected so that respiratory gating simulations could be performed. Breathing data was obtained by tracking an external surrogate positioned on the patient's upper abdomen in the same position that was used for 4DCT imaging at simulation. In total, 151 CBCT scans were acquired, including 105 routine scans with compression from 19 patients. For 11 of those patients, 46 additional scans were acquired without compression moments before the compressed scan, with three patients having 1, 2, and 3 uncompressed scans, and the remaining eight patients having 5 uncompressed scans.

Tumor motion reconstruction

A two-part, in-house routine developed and implemented in MATLAB (Mathworks, Natick, MA) was used to track fiducial markers in CBCT projection images and then reconstruct the 3D trajectory that occurred during each CBCT scan, both of which have been described elsewhere [20,21]. In brief, the fiducial marker tracking component of the routine automatically tracks markers with an iterative routine that reconstructs the cluster of markers, creates template images based on this reconstruction, then uses template-matching to track and stabilize markers in projection images. Reconstructing stabilized images provides a higher quality reconstruction of the cluster of markers, which provides better template images, and allows for improved template-matching. Repeated iterations of this loop converge upon a high quality set of template images and accurate tracking of the marker cluster.

The 3D trajectory reconstruction routine is briefly described as follows. The method takes 2D positions seen in CBCT projection images and sorts these tracked position according to breathing phase as determined by superior-inferior position. Then, 3D Gaussian probability distribution functions were computed for each breathing phase. Using these probability distributions, the depth position of the marker cluster in each projection image was deemed to be the position of maximum probability along the line between the kV x-ray source and the imaging panel. In this fashion, 3D target motion was determined from all CBCT scans.

Simulated respiratory gating

For each uncompressed CBCT scan, target motion was evaluated for two scenarios: no motion mitigation, and respiratory gating. For the no motion mitigation scenario, target motion was simply the motion determined by the tumor motion reconstruction technique. For the respiratory gating scenario, target motion was determined via simulation according to the position of the external surrogate. Using a typical 40% duty cycle, respiratory gating motion was calculated as a subset of unmitigated motion data by discarding instances when the position of the external surrogate was greater than its 40^{th} percentile value [22]. As such, gating assumes a strong correlation between the positions of the external surrogate and the internal target.

Simulated reduced margins

To evaluate the clinical impact of motion mitigation, a simulated clinical scenario was used to evaluate target coverage. Motion was assessed by determining how consistently targets

stayed within reduced margins relative to their average position. The ITV used during actual treatment encompassed the entire range of motion observed during the 4DCT scan at simulation, and this volume was also expanded by the physician on a case-by-case basis to create the PTV. In the reduced margins scenario, PTVs were created by expanding the CTV at its mean position using uniform margins of 2 mm in left-right (LR) and anterior-posterior (AP) directions, and 3 mm in the superior-inferior (SI) direction. Daily coverage rates were calculated as the percentage of time that targets remained within these set margins. This simulation assumes that patients were perfectly aligned according to the average target position in each motion mitigation setup.

Statistical methods

Average values for daily range of motion and daily coverage were calculated by first calculating mean values across all treatment fractions for each patient, and then calculating mean values across all patients. Maximum and minimum values were selected from daily measurements for all patients. Statistical significances of any differences between motion mitigation scenarios were calculated by only using data from fractions where all three scenarios (no mitigation, abdominal compression, respiratory gating) were evaluated (i.e., n=46), and were calculated independently for LR/AP/SI directions using Wilcoxon's Signed-Rank test (paired, two-tailed, significance level $p<0.01$).

Results

Daily tumor motion

Average (minimum-maximum) daily motion ranges for no mitigation, abdominal compression, and respiratory gating are shown in Table 1. Compared to no mitigation, abdominal compression significantly reduced daily target motion in AP and SI directions by 2 and 5.4 mm, respectively. However, compression did not significantly reduce target motion in the LR direction ($p=0.88$). Respiratory gating significantly reduced target motion in LR/AP/SI directions by 2.1, 3.4, and 8.4 mm, respectively. Gating was also significantly more effective than compression at reducing target motion in all directions.

For the 46 treatment fractions where all three scenarios were evaluated, Figure 1 shows daily ranges of motion for compression and gating plotted with respect to their corresponding daily ranges of motion observed without motion mitigation. Figure 2 shows relative probability distributions for all patients with respect to the median position at 0. For easier visual comparison, distributions were normalized to share a common maximum value (i.e., area under each curve varies), but areas to the left and right of 0 are equal for each distribution. For no mitigation, 95% of motion (i.e., 2.5^{th}-97.5^{th} percentiles) in LR/AP/SI directions remained within spans of 5.0, 5.7, and 11.9 mm, respectively. For abdominal compression, these values were 4.2, 4.3, and 7.9 mm, and for respiratory gating, these values were 3.1, 3.2, and 4.6 mm, respectively. In addition, motion with gating was more symmetrical, with no mitigation and abdominal compression distributions slanting more towards end-exhalation positions (i.e., posterior and superior).

Reduced internal margins

The effectiveness of compression and gating at reducing tumor motion was largely reflected in their ability to improve target coverage rates (see Table 2, Figure 3). Compared against no mitigation, compression did not significantly improve coverage rates in the LR direction ($p=0.33$), but did significantly improve coverage rates by 11% and 25% in AP and SI directions, respectively. Gating significantly improved coverage rates in LR/AP/SI directions by 8%, 16%, and 36%, respectively. As was seen with motion reduction, gating provided coverage rates significantly better than abdominal compression in all directions. When considering all 19 patients, the symmetrical margins necessary to encompass 95% of the target motion in LR/AP/SI directions were 3/4/7 mm for the no motion mitigation scenario, 3/3/5 mm for abdominal compression, and 2/2/3 mm for respiratory gating.

Discussion

This work demonstrates that, for pancreatic SBRT, respiratory gating achieved greater reductions in target motion than abdominal compression. This decreased motion also translated into potential reductions in target volume expansion. Although previous studies have investigated these approaches individually, none have compared them side-by-side with the same group of patients. When examining these approaches separately, discerning their comparative efficacies is difficult. One must rely on comparing the average range of motion for a group of patients using one technique against the average range of motion for a separate group of patients using the other technique. In a prior study, we showed that pancreatic tumor motion can vary significantly from patient to patient [18]. As such, statistically significant differences can easily be lost when comparing separate groups of patients. Nevertheless, the following discussion examines where the current work fits amongst previous studies.

Prior works have examined abdominal tumor motion with and without abdominal compression to evaluate its efficacy. A study by Heinzerling *et al* that focused on stereotactic treatment of the lung and liver also examined motion of nearby organs for 10 patients [23]. They found that compression significantly reduced overall motion of the pancreas by ~33%. More recently, Lovelock *et al* looked at 42 abdominal cancer patients, 3 of which had pancreatic cancer [24]. Using fluoroscopic imaging, they found that compression reduced average (range) target motion in the SI direction from 11.4 (5-20) to 4.4 (1-8) mm. Although the average range of compressed motion seen in their work was lower than the range seen in the current work (8.5 mm), this is likely due to differences in procedures. Lovelock *et al* used pre-simulation fluoroscopic imaging to select a level of compression that would ensure SI motion <5 mm. If this was not achieved and the patient was willing, pressure was increased. In the current work, no pre-simulation imaging with compression was acquired; compression pressure was increased until the patient began to feel discomfort. Thus, patients may be more amenable to additional pressure if they know that a certain range of motion is being sought. For compressed treatments, if a maximum acceptable range of motion is specified, pre-simulation fluoroscopic imaging should be used to ensure that sufficient pressure is applied.

Regarding respiratory gating, a recent work by Heerkens *et al* used MRI to observe pancreatic tumor motion [25]. For 15 patients, averages (ranges) of target motion without gating were 3 (2-5), 5 (1-13) and 15 (6-34) mm in LR/AP/SI directions, respectively. For 11 of those patients, simulated respiratory gating with a 50% duty cycle was sufficient to ensure total coverage using 5 mm margins. Another recent work by Huguet *et al* used 4DCT imaging to measure target motion and simulate gating for 36 pancreatic cancer patients [26]. They saw average±SD ranges of motion of 3±2, 6±3, and 13±7 mm in LR/AP/SI directions, respectively. By gating around end-exhalation, these ranges of motion could be reduced by 46-60%. This is corroborated by the reductions in LR/AP/SI motion observed in this work (40%, 47%, 60%, respectively).

Although our evaluation of coverage rates offers useful insight into the feasibility of margin reductions for pancreatic SBRT, it should be emphasized that the scenario presented here is overly simplistic. It only considers the margins necessary to account for motion. It assumes perfect target localization and re-alignment before treatment. It assumes that no positional baseline shifts occur during each treatment, and that fiducial markers do not migrate before the last fraction is delivered. Changes in tumor trajectories seen in each motion scenario—a topic worthy of its own study—were ignored, reduced to simple ranges of motion. All of these factors must be considered when defining margins. Nevertheless, understanding how motion alone can affect coverage rates allows for well-informed margin selection.

Additionally, the dispersed nature of data in Figure 1 highlights two important points worth consideration. First, target motion can vary by the minute; this is particularly evident in plots of compressed motion in the LR direction (i.e., the direction unaffected by compression). Second, the correlation between an external surrogate and the internal target only accounts for respiratory motion. As such, respiratory gating would most likely benefit from continually tracking the target directly.

Conclusion

Using pre-treatment imaging, daily target motion was evaluated in order to examine the efficacy of abdominal compression and respiratory gating. Compared to no motion mitigation, abdominal compression significantly reduced motion in AP and SI directions by 27% and 39%, respectively. However, respiratory gating was significantly better, reducing LR/AP/SI motion by 40%, 47%, and 60%, respectively. Hence, respiratory gating was shown to be the most effective strategy for reducing target motion in pancreatic SBRT.

Acknowledgments

This work was funded in part by the National Institutes of Health (K12CA086913), by the University of Colorado Cancer Center/American Cancer Society institutional research grant #57-001-53, by an award from the Boettcher Foundation, and by a research grant from Varian Medical Systems. These funding sources had no involvement in the study design; in the collection, analysis, and interpretation of data; in the writing of the manuscript; or in the decision to submit the manuscript for publication.

References

1. Hammel P, Huguet F, van Laetham J, et al. Effect of Chemoradiotherapy vs Chemotherapy on Survival in Patients With Locally Advanced Pancreatic Cancer Controlled After 4 Months of

Gemcitabine With or Without ErlotinibThe LAP07 Randomized Clinical Trial. JAMA. 2016; 315(17):1844–1853. [PubMed: 27139057]

2. Rwigema JCM, Parikh SD, Heron DE, et al. Stereotactic body radiotherapy in the treatment of advanced adenocarcinoma of the pancreas. Am J Clin Oncol. 2011; 34:63–69. [PubMed: 20308870]
3. Chuong MD, Springett GM, Freilich JM, et al. Stereotactic body radiation therapy for locally advanced and borderline resectable pancreatic cancer is effective and well tolerated. Int J Radiat Oncol Biol Phys. 2013; 86:516–522. [PubMed: 23562768]
4. Trakul N, Koong AC, Chang DT. Stereotactic body radiotherapy in the treatment of pancreatic cancer. Semin Radiat Oncol. 2014; 24:140–147. [PubMed: 24635871]
5. Hajj C, Goodman KA. Pancreatic cancer and SBRT: a new potential option? Rep Pract Oncol Radiother. 2015; 20:377–384. [PubMed: 26549996]
6. Goodman KA. Stereotactic body radiation therapy for pancreatic cancer. Cancer J. 2016; 22:290–295. [PubMed: 27441749]
7. Koong AC, Christofferson E, Le QT, et al. Phase II study to assess the efficacy of conventionally fractionated radiotherapy followed by a stereotactic radiosurgery boost in patients with locally advanced pancreatic cancer. Int J Radiat Oncol Biol Phys. 2005; 63:320–323. [PubMed: 16168826]
8. Mahadevan A, Miksad R, Goldstein M, et al. Induction gemcitabine and stereotactic body radiotherapy for locally advanced nonmetastatic pancreas cancer. Int J Radiat Oncol Biol Phys. 2011; 81:e615–e622. [PubMed: 21658854]
9. Brunner TB, Nestle U, Grosu AL, Partridge M. SBRT in pancreatic cancer: what is the therapeutic window? Radiother Oncol. 2015; 114:109–116. [PubMed: 25466369]
10. Hoyer M, Roed H, Sengelov L, et al. Phase-II study on stereotactic radiotherapy of locally advanced pancreatic carcinoma. Radiother Oncol. 2005; 76:48–53. [PubMed: 15990186]
11. Sanders MK, Moser AJ, Khalid A, et al. EUS-guided fiducial placement for stereotactic body radiotherapy in locally advanced and recurrent pancreatic cancer. Gastrointest Endosc. 2010; 71:1178–1184. [PubMed: 20362284]
12. Lens E, van der Horst A, Versteijne E, Bel A, van Tienhoven G. Considerable pancreatic tumor motion during breath-holding. Acta Oncologica. 2016; 55:1360–1368. [PubMed: 27583771]
13. Kupelian P, Willoughby T, Mahadevan A, et al. Multi-institutional clinical experience with the Calypso system in localization and continuous, real-time monitoring of the prostate gland during external radiotherapy. Int J Radiat Oncol Biol Phys. 2007; 67:1088–1098. [PubMed: 17187940]
14. Keall PJ, Ng JA, O'Brien R, et al. The first clinical treatment with kilovoltage intrafraction monitoring (KIM): a real-time image guidance method. Med Phys. 2015; 42:354–358. [PubMed: 25563275]
15. Minn AY, Schellenberg D, Maxim P, et al. Pancreatic tumor motion on a single planning 4D-CT does not correlate with intrafraction tumor motion during treatment. Am J Clin Oncol. 2009; 32:364–368. [PubMed: 19398901]
16. Ge J, Santanam L, Noel C, Parikh PJ. Planning 4-dimensional computed tomography (4DCT) cannot adequately represent daily intrafractional motion of abdominal tumors. Int J Radiat Oncol Biol Phys. 2013; 85:999–1005. [PubMed: 23102840]
17. Lens E, van der Horst A, Kroon PS, et al. Differences in respiratory-induced pancreatic tumor motion between 4D treatment planning CT and daily cone beam CT, measured using intratumoral fiducials. Acta Oncol. 2014; 53:1257–1264. [PubMed: 24758251]
18. Jones BL, Schefter T, Miften M. Adaptive motion mapping in pancreatic SBRT patients using Fourier transforms. Radiother Oncol. 2015; 115:217–222. [PubMed: 25890573]
19. Rankine L, Wan H, Parikh P, et al. Cone-beam computed tomography internal motion tracking should be used to validate 4-dimensional computed tomography for abdominal radiation therapy patients. Int J Radiat Oncol Biol Phys. 2016; 95:818–826. [PubMed: 27020102]
20. Jones BL, Westerly D, Miften M. Calculating tumor trajectory and dose-of-the-day using cone-beam CT projections. Med Phys. 2015; 42:694–702. [PubMed: 25652483]
21. Campbell WG, Miften M, Jones BL. Automated target tracking in kilovoltage images using dynamic templates of fiducial marker clusters. Med Phys. 2017; 44:364–374. [PubMed: 28035655]

22. Vedam SS, Keall PJ, Kini VR, Mohan R. Determining parameters for respiration-gated radiotherapy. Med Phys. 2001; 28:2139–2146. [PubMed: 11695776]

23. Heinzerling JH, Anderson JF, Papiez L, et al. Four-dimensional computed tomography scan analysis of tumor and organ motion at varying levels of abdominal compression during stereotactic treatment of lung and liver. Int J Radiat Oncol Biol Phys. 2008; 70:1571–1578. [PubMed: 18374231]

24. Lovelock DM, Zatcky J, Goodman K, Yamada Y. The effectiveness of a pneumatic compression belt in reducing respiratory motion of abdominal tumors in patients undergoing stereotactic body radiotherapy. Technol Cancer Res Treat. 2014; 13:259–267. [PubMed: 24206202]

25. Heerkens HD, van Vulpen M, van den Berg CAT, et al. MRI-based tumor motion characterization and gating schemes for radiation therapy of pancreatic cancer. Radiother Oncol. 2014; 111:252–257. [PubMed: 24746577]

26. Huguet F, Yorke ED, Davidson M, et al. Modeling pancreatic tumor motion using 4-dimensional computed tomography and surrogate markers. Int J Radiat Oncol Biol Phys. 2015; 91:579–587. [PubMed: 25680600]

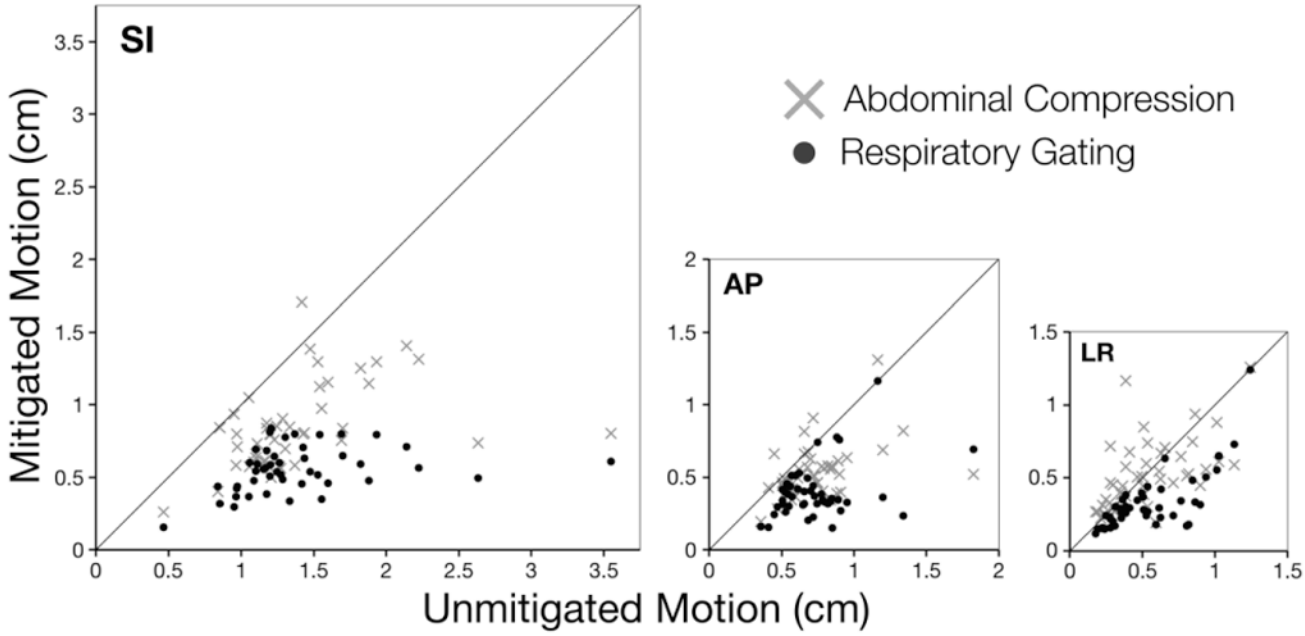

Fig. 1.

For 46 treatment fractions, motion was evaluated for three scenarios: no mitigation, abdominal compression, and respiratory gating. Here, daily ranges of mitigated motion (i.e., abdominal compression or respiratory gating) are plotted with respect to daily ranges of unmitigated motion in SI, AP, and LR directions. Solid lines in each chart have a slope of 1, roughly indicating where points would vertically shift to without motion mitigation.

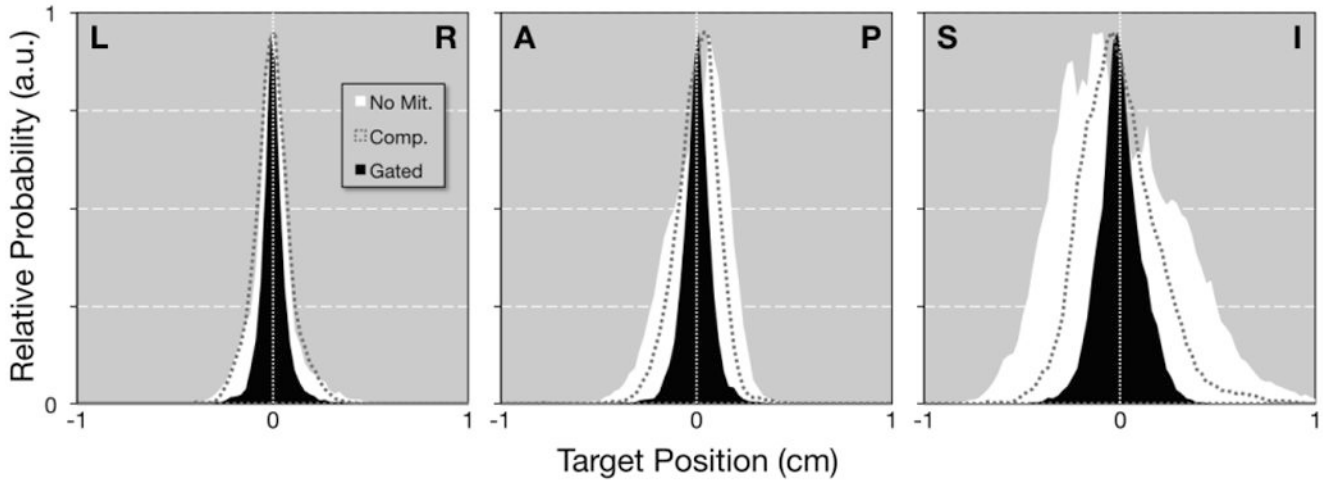

Fig. 2.

Probability distributions are shown for LR, AP, and SI directions and three scenarios: no mitigation (white area), abdominal compression (dashed gray line), and respiratory gating (black area). To aid visual comparison, distributions are plotted relative to their median value at 0, and the maximum value in each distribution has been normalized to a shared value of 0.95.

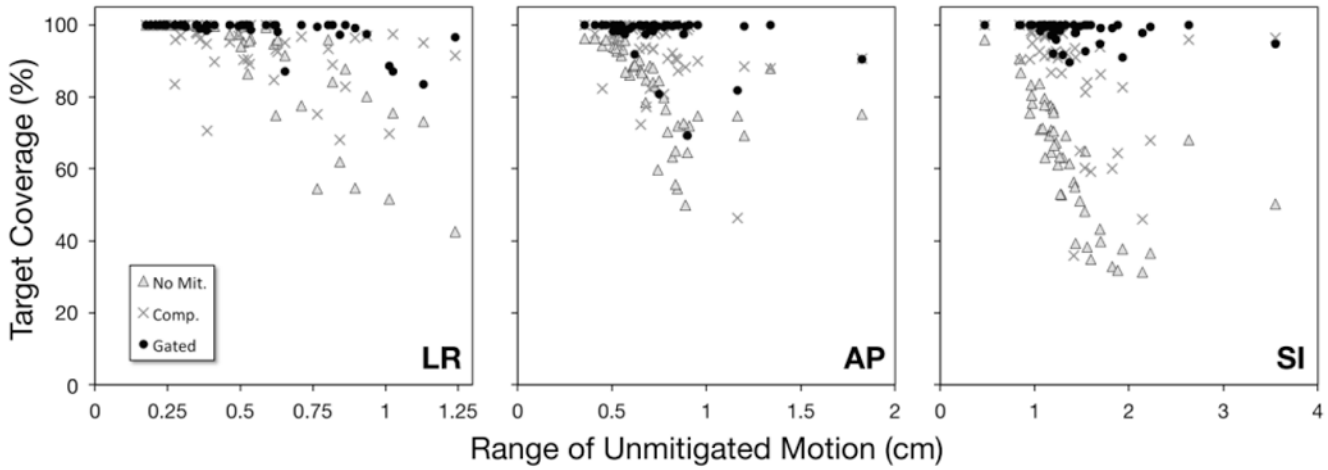

Fig. 3.

Daily rates of target coverage with reduced internal margins (2 mm for LR and AP, 3 mm for SI) are plotted with respect to daily ranges of unmitigated motion for LR, AP, and SI directions and three scenarios: no mitigation (grey Δs), abdominal compression (grey ×s), and respiratory gating (black •s).

Table 1

Daily target motion ranges (peak-to-peak) are shown for LR, AP, and SI directions for three motion mitigation scenarios. Values shown are **mean** [minimum – maximum] given in cm.

(cm)	LR	AP	SI
No motion mitigation	**0.53** [0.18 – 1.24]	**0.73** [0.35 – 1.82]	**1.39** [0.47 – 3.55]
Abdominal compression	**0.52** [0.13 – 1.37]	**0.53**† [0.19 – 1.31]	**0.85**† [0.16 – 1.71]
Respiratory gating	**0.32**‡ [0.12 – 1.24]	**0.39**‡ [0.15 – 1.16]	**0.55**‡ [0.15 – 0.84]

†significantly lower ($p<0.01$) than no motion mitigation

‡significantly lower ($p<0.01$) than both no motion mitigation and abdominal compression

Table 2

In a simulated clinical scenario with reduced internal margins (2 mm for LR and AP, 3 mm for SI), daily coverage values are shown for three motion mitigation scenarios. Values shown are **mean** [minimum – maximum] given in %.

(%)	LR	AP	SI
No motion mitigation	**90.3** [42.6 – 100]	**82.0** [49.9 – 97.0]	**62.2** [31.4 – 96.0]
Abdominal compression	**93.5** [68.1 – 100]	**93.0**† [46.3 – 100]	**87.6**† [35.9 – 100]
Respiratory gating	**98.5**‡ [83.5 – 100]	**97.7**‡ [69.2 – 100]	**98.3**‡ [89.6 – 100]

†significantly lower ($p<0.01$) than no motion mitigation

‡significantly lower ($p<0.01$) than both no motion mitigation and abdominal compression